Phosphine-Induced Phase Transition in Copper Sulfide Nanoparticles Prior to Initiation of a Cation Exchange Reaction

Benjamin C. Steimle, 1 Robert W. Lord, 1 Raymond E. Schaak 1,2,3*

¹ Department of Chemistry, ² Department of Chemical Engineering, and ³ Materials Research Institute, The Pennsylvania State University, University Park, PA 16802

Supporting Information Placeholder

ABSTRACT: Cation exchange reactions of colloidal copper sulfide nanoparticles are widely used to produce derivative nanoparticles having unique compositions, metastable crystal structures, and complex heterostructures. The copper sulfide crystal structure plays a key role in the mechanism by which cation exchange occurs and the product that forms. Here, we show that digenite copper sulfide nanoparticles undergo a spontaneous phase transition to tetragonal chalcocite in situ, prior to the onset of cation exchange. Roomtemperature sonication of digenite (Cu₁₈S) in trioctylphosphine, a Lewis base that drives cation exchange, extracts sulfur to produce tetragonal chalcocite (Cu₂S). The subtle structural differences between digenite and tetragonal chalcocite are believed to influence the accessibility of cation diffusion channels, and concomitantly the mechanism of cation exchange. Structural relationships in nanocrystal cation exchange are therefore dynamic, and intermediates generated in situ must be considered.

Chemical reactions that transform one type of nanoparticle into another have emerged as powerful tools for generating otherwise inaccessible products in a rational manner. Such reactions retain key property-defining nanoparticle features, ultimately providing chemical pathways for controllably synthesizing designer nanoparticles for catalysis, photovoltaics, optoelectronics, photon up-conversion, and ratiometric sensing. Colloidal nanoparticle cation exchange reactions, whereby cations in a template nanoparticle are replaced by cations from solution, are especially powerful. Omplete cation exchange can produce nanoparticles with otherwise inaccessible compositions, morphologies, and crystal structures, I1-I5 while partial cation exchange can produce libraries of sophisticated and complex heterostructured nanoparticles.

Most nanoparticle cation exchange reactions retain aspects of the template crystal structure in the product. For example, roxbyite copper sulfide, Cu_{1.8}S, has a distorted hexagonally close packed (HCP) anion sublattice, and the cation exchange products are typically HCP-based wurtzite phases. ^{13,18,19} For digenite copper sulfide, which has the same nominal composition but a different cubic close packed (CCP) anion sublattice, cation exchange reactions instead produce CCP-based zincblende phases. ^{19,20} Crystal structure retention is also important in partial cation exchange reactions, where persistence of the continuous anion sublattice allows epitaxial interfaces to form in certain crystallographic directions. ^{18,21,22}

Crystal structure is also important in the two primary mechanisms of nanoparticle cation exchange: (1) guest cation diffusion through unoccupied interstitial sites followed by host cation release²³ and (2) guest cation exchange at the nanoparticle surface

followed by hopping through vacant cation sites. ²⁴ Both mechanisms require cation diffusion that occurs sufficiently rapidly that the anion sublattice is comparatively rigid. The cation diffusion pathway through the crystal, and also its diffusion rate, therefore depends on the crystal structure, which defines the coordination environments and accessibility of the interstitial and vacant sites. ^{25–27} The formation of unique nanoparticle products exploits and requires this involvement of the crystal structure in the mechanism.

The proposed mechanisms of nanoparticle cation exchange that result in retention of crystal structure assume that the structure is invariant throughout the process. Here, we challenge this key assumption by showing that the crystal structure of the template nanoparticle can change *in situ* prior to cation exchange. We show that digenite copper sulfide (Cu_{1.8}S) undergoes a rapid *in situ* transformation to tetragonal chalcocite (Cu₂S) under common reaction conditions, prior to initiation of cation exchange. It is therefore the tetragonal chalcocite intermediate that actually undergoes cation exchange, rather than digenite. The mechanism by which crystal structure retention occurs must therefore consider the tetragonal chalcocite intermediate as the structure-defining species.

Consider the exchange of the Cu⁺ cations in digenite with Zn²⁺ to produce zincblende ZnS, which is known to retain both anion and cation sublattice structures (Figure 1a).¹⁹ Here, cation exchange is driven by trioctylphosphine (TOP),⁹ a soft base that coordinates to the outgoing Cu⁺ cations to help facilitate the incorporation of cations from solution into the nanoparticle. The well-established protocol for such reactions (Figure S1) involves first sonicating or dispersing the template nanoparticles in TOP at room temperature under an inert atmosphere. ^{16–22,37} TOP is believed to function as a coordinating ligand and solvent at this stage, before the entire suspension is introduced to the exchanging cation. However, X-ray diffraction (XRD) data for aliquots removed during room-temperature TOP sonication revealed that the digenite nanoparticles began transforming to tetragonal chalcocite within one minute, and they completely converted within 45 minutes (Figure 1b).

The XRD pattern for the as-synthesized copper sulfide particles (Figure 1b) matched well with PDF card 00-047-1758, ²⁸ which corresponds to digenite. This reference XRD pattern, labeled in the PDF database as rhombohedral digenite, can be traced to a low-temperature digenite phase that can be described by a cubic superstructure that has the same CCP sulfur sublattice and nominal cation coordination as cubic digenite but with subtly different cation ordering, ²⁹ which results in additional weak XRD reflections (Figure S2). ^{29,30} Cubic digenite is known to undergo a spontaneous, reversible transition to rhombohedral digenite upon cooling below ~70 °C, ^{31,32} then possibly transition to a low-temperature cubic

structure.²⁹ Many digenite nanoparticle samples^{20,33–35} therefore contain reflections from rhombohedral digenite or the related low-temperature cubic superstructure, analogous to ours. After sonicating this digenite sample for 1 minute in TOP, peaks for tetragonal chalcocite began to appear, and by 45 minutes, the pattern transformed entirely to tetragonal chalcocite. Reflections at 37° and 49° 20, representing an additional unidentified impurity, persisted unchanged throughout all samples, and therefore are not relevant to the cation exchange process.

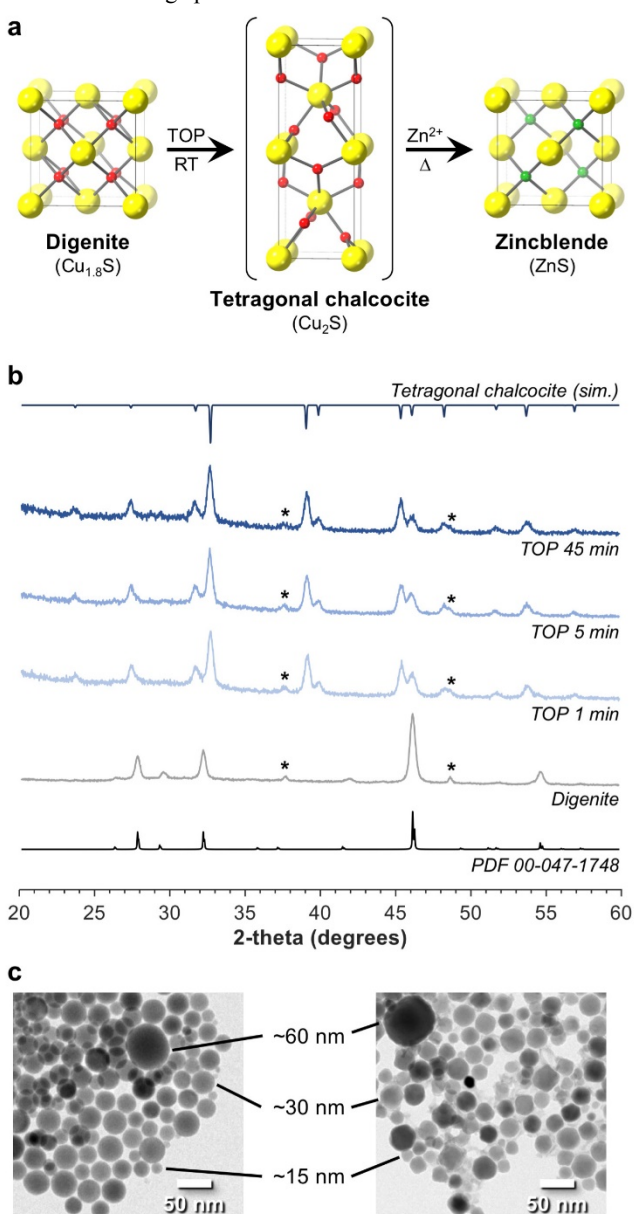


Figure 1. (a) Transformation of digenite to a tetragonal chalcocite intermediate prior to forming a zincblende product through cation exchange. (b) XRD patterns for the digenite precursor and after sonicating in TOP for various times. PDF 00-047-1748 (digenite) and a simulated tetragonal chalcocite pattern are shown for comparison. The asterisk (*) labels a persistent impurity. (c) TEM images for digenite and tetragonal chalcocite show retention of size distribution and morphology.

After 45 min in TOP

(tetragonal chalcocite Cu2S)

As-synthesized

(digenite Cu_{1.8}S)

This *in situ* conversion of digenite to tetragonal chalcocite is rationalized by the known ability of TOP to extract sulfur from metal

sulfide particles and transform them to more metal-rich sulfides, driven by the formation of the TOP=S complex. ^{36,37} This behavior, mediated by tributylphosphine rather than TOP, has also been used to transform roxbyite Cu_{1.8}S to the more metal-rich copper sulfides djurleite (Cu_{1.94}S) and low-chalcocite (Cu₂S). ³⁷ Additionally, TOP is thought to reduce the cation defect density in Cu₂Se at elevated temperatures, decreasing the rate of cation exchange. ²⁵ This transformation reaction, however, has not been implicated in the mechanism by which cation exchange occurs nor applied to structure retention relationships.

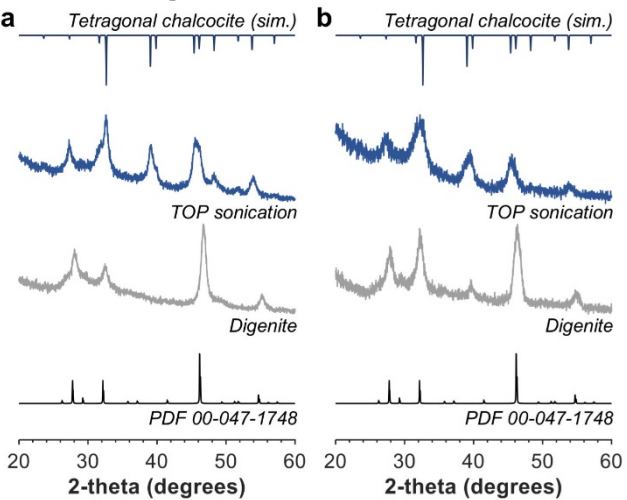


Figure 2. XRD patterns demonstrating the TOP-induced phase transition in different samples of digenite: (a) faceted ~ 20 -nm particles and (b) ~ 10 nm particles. PDF 00-047-1748 (digenite) and a simulated tetragonal chalcocite pattern are shown for comparison.

For this initial aliquot study, our digenite sample contained a trimodal mixture of ~15-, ~30-, and ~60-nm particles (Figures 1c, S3). Large (>20-nm) particles, which were only accessible as part of a mixed-population sample, helped ensure sufficiently sharp XRD peaks for reliable phase analysis. However, samples with multiple crystallite sizes can complicate XRD analysis. Simulated XRD patterns (Figure S4) help confirm that each subpopulation undergoes the phase transformation. The trimodal sample was beneficial, however, for TEM analysis. TEM images of the particles assynthesized and after 45 minutes in TOP revealed that the three particle sizes remained (Figure 1c), providing confidence that the conversion of digenite to tetragonal chalcocite was due to a phase transformation rather than dissolution and reprecipitation.

The trimodal digenite sample contains larger particles than those most often used for cation exchange reactions. Therefore, we also synthesized, using different reaction conditions, a sample with particle sizes less than 20 nm (Figures 2a, S5). A similar in situ TOPinduced transformation from digenite to tetragonal chalcocite was also observed for this sample. When these tetragonal chalcocite nanoparticles react with excess Zn²⁺ at 120 °C for 30 minutes in the presence of TOP, the cation exchange product is zincblende ZnS (Figure S6), which is the product expected from cation exchange of digenite using similar conditions.¹⁹ We also synthesized 10-nm digenite particles to confirm that size and morphological heterogeneity do not influence the in situ phase transformation (Figures 2b, S5). While the XRD pattern has significant size-dependent peak broadening, the digenite peaks still change in intensity and shift to match those expected for tetragonal chalcocite after sonicating for 60 minutes in TOP.

It is important to understand the crystallographic relationships among digenite, tetragonal chalcocite, and zincblende. Cubic digenite, rhombohedral digenite, and the low-temperature cubic digenite superstructure, as mentioned previously, comprise a majority of the as-synthesized particles. All of these digenite-related phases are cation-deficient (Cu_{1.8}S) copper sulfides having a CCP

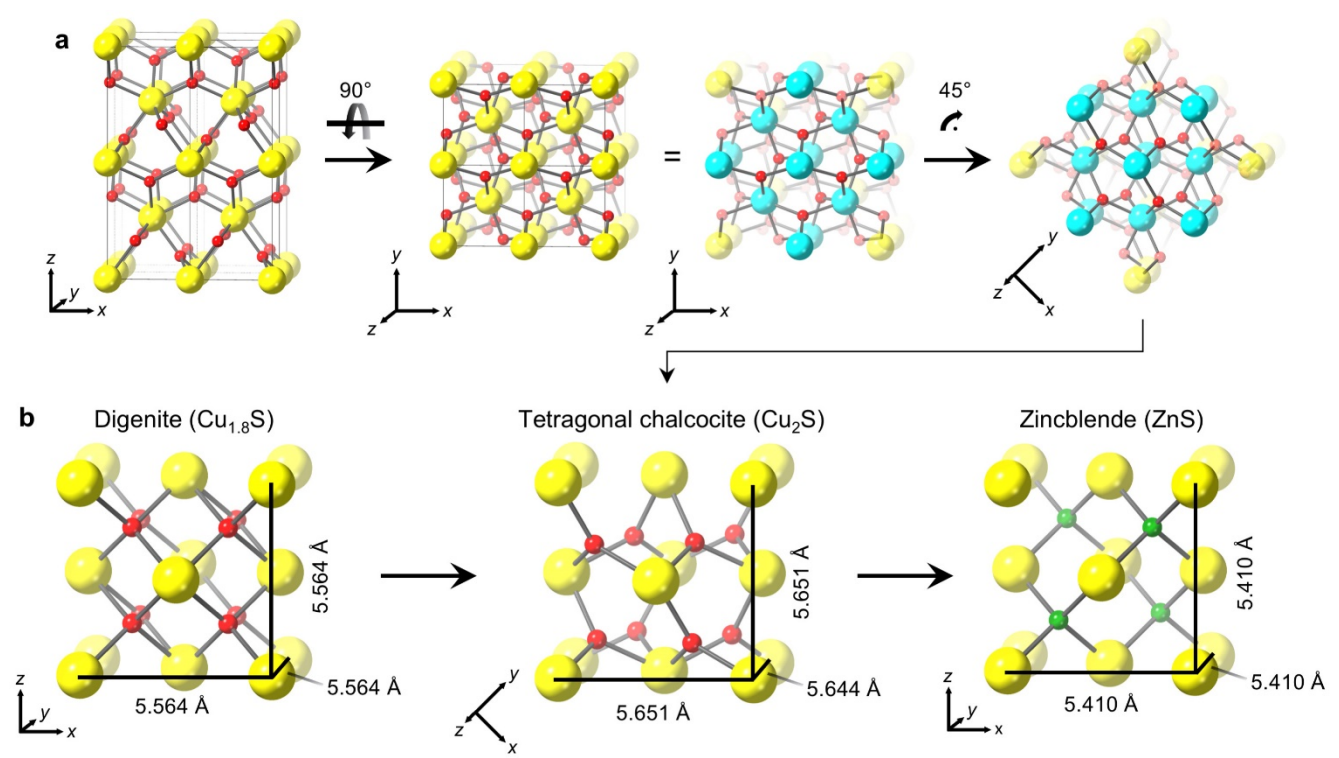


Figure 3. (a) Crystallographic projections highlighting the digenite-like FCT subunit within tetragonal chalcocite (copper = red, sulfur = yellow). (b) Crystal structure relationships among digenite, tetragonal chalcocite, and zincblende, showing the intersulfur spacings.

anion sublattice with nearly identical inter-sulfur spacings and highly mobile Cu⁺ cations. ^{28,36} In cubic digenite, Cu⁺ occupies most of the tetrahedral holes and can easily move among a variety of sites, ³⁰ while rhombohedral digenite and the low-temperature cubic superstructure have Cu⁺ cations that occupy numerous different holes such that there are ordered cation vacancies. ^{28–31} These phases differ only subtly based on cation ordering and positioning, so we consider cubic digenite, the simplest of the structures, for the comparisons that follow.

In contrast to digenite, tetragonal chalcocite is a stoichiometric (Cu₂S) copper sulfide having a body-centered tetragonal (BCT) anion sublattice and trigonally-coordinated Cu⁺ cations. The structure of tetragonal chalcocite is substantially different from that of lowand high-chalcocite, which have similar names but an anion sublattice that is nominally HCP, 38 rather than BCT. A face-centered tetragonal (FCT) sublattice can be defined within tetragonal chalcocite to more easily compare it to digenite (Figure 3a). The FCT sublattice in tetragonal chalcocite has dimensions of 5.651 Å, 5.651 Å, and 5.644 Å, which are all slightly larger than the 5.564-Å lattice parameter of cubic digenite (Figure 3b). To form tetragonal chalcocite from digenite, sulfur is extracted by TOP and then the sulfur sublattice must expand in all directions while the Cu⁺ coordination shifts from tetrahedral to trigonal planar, creating vacant tetrahedral interstitial sites. This phase transition has been observed previously when thermally annealing cubic and rhombohedral digenite nanoparticles, indicating that tetragonal chalcocite is more thermodynamically stable.³⁹ The anion sublattices of both digenite and tetragonal chalcocite are similar to the FCC sublattice of zincblende, where cations occupy half of the tetrahedral sites. Considering the structural similarities, the formation of a zincblende product upon Zn²⁺ exchange is expected, as the Zn²⁺ can insert into the vacant tetrahedral interstitial sites of tetragonal chalcocite.

The structural differences between digenite and tetragonal chalcocite may influence the pathway by which zincblende forms. Digenite is a cation-deficient phase that, at the temperatures used for cation exchange, has a high symmetry cubic space group (Fm-3m) and unoccupied octahedral interstitial sites that could serve as diffusion channels in any of the six <110> directions (Figure 4). Upon transitioning to lower-symmetry (P4₃2₁2) tetragonal chalcocite, which is stoichiometric, there is no longer a significant concentration of cation vacancies. Tetragonal chalcocite has unoccupied tetrahedral and octahedral interstitial sites, forming large diffusion channels accessible only in the [100] and [010] directions and inaccessible in the [114], [11-4], [1-14], and [-114] directions, all six of which are structurally related to the <110> directions in digenite (Figure 4). This reduces the number of cation diffusion pathways from the six equivalent <110> directions digenite to only two in tetragonal chalcocite. Therefore, the cation exchange mechanism for tetragonal chalcocite is inherently different than for digenite. Cation diffusion into tetragonal chalcocite is likely to be based entirely on interstitial sites compared to digenite, which could proceed through both interstitial sites and vacant cation sites. Additionally, interstitial-based diffusion channels in tetragonal chalcocite are only accessible in two crystallographic directions, which would strongly influence the types of heterostructured nanoparticles that are accessible using partial cation exchange.

Transient solid-state intermediates have been shown to affect the outcomes of some other colloidal nanoparticle reactions. In the one-pot synthesis of certain metastable ternary metal sulfides, structurally-related binary phases form *in situ* as reactive intermediates before transforming through cation exchange processes. 40,41 Copper sulfide phase transitions have also been observed during partial cation exchange reactions. 42 These phase transitions

mitigate interfacial strain, but only after cation exchange has commenced, and therefore not in a way that influences the mechanism. The observation here that the copper sulfide structure changes *before* cation exchange commences is distinct from these previous reports and has important implications for understanding structure retention and reaction pathways during such reactions.

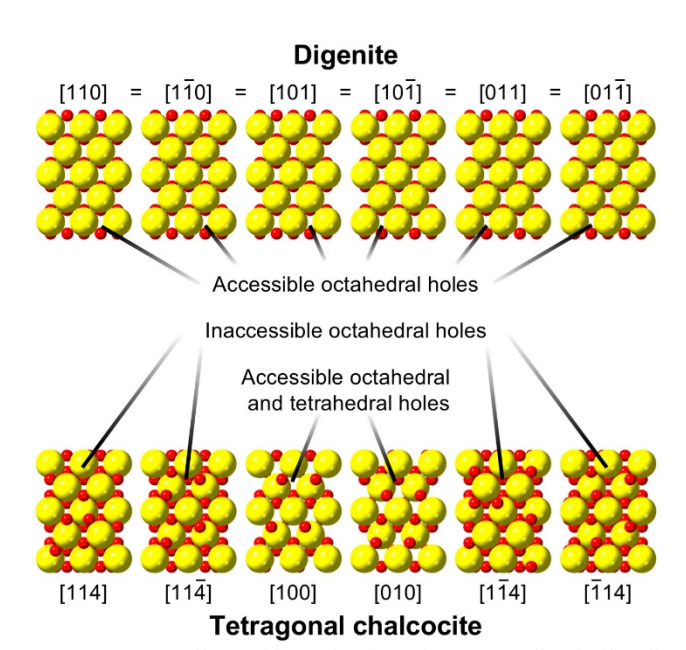


Figure 4. Crystallographic projections, in structurally-similar directions, for digenite and tetragonal chalcocite. In digenite, all <110> directions are equivalent and octahedral holes are accessible in all six directions. In tetragonal chalcocite, Cu⁺ shifts to trigonal holes, leaving vacant tetrahedral and octahedral holes that are only accessible in the [100] and [010] directions and are blocked by Cu⁺ cations in the other four, structurally similar directions. Sulfur = yellow, copper = red.

The discovery that a prototypical cation exchange process in a commonly studied system proceeds through a previously unrecognized intermediate with a crystal structure that is distinct from both the precursor and the product has important implications for predicting, understanding, modeling, controlling, and applying nanoparticle cation exchange reactions. This is especially significant given the role of crystal structure in templating metastable phases, inducing heterostructuring and interface formation, and defining the cation exchange mechanism.

ASSOCIATED CONTENT

Supporting Information

The Supporting Information is available free of charge on the ACS Publications website.

Complete materials and methods, additional XRD and TEM characterization, details on the crystal structure information used to generate crystal structures and simulated XRD patterns and references 43-45.

AUTHOR INFORMATION

Corresponding Author

*res20@psu.edu

Notes

The authors declare no competing financial interests.

ACKNOWLEDGMENT

This work was supported by the U.S. National Science Foundation under grant DMR-1904122. TEM imaging was performed at the Materials Characterization Lab of the Penn State Materials Research Institute.

REFERENCES

- (1) Buck, M. R.; Schaak, R. E. Emerging Strategies for the Total Synthesis of Inorganic Nanostructures. *Angew. Chem. Int. Ed.* **2013**, *52*, 6154–6178
- (2) Chandrasekaran, S.; Yao, L.; Deng, L.; Bowen, C.; Zhang, Y.; Chen, S.; Lin, Z.; Peng, F.; Zhang, P. Recent Advances in Metal Sulfides: From Controlled Fabrication to Electrocatalytic, Photocatalytic and Photoelectrochemical Water Splitting and Beyond. *Chem. Soc. Rev.* **2019**, *48*, 4178–4280
- (3) Wang, Y.-X.; Wei, M.; Fan, F.-J.; Zhuang, T.-T.; Wu, L.; Yu, S.-H.; Zhu, C.-F. Phase-Selective Synthesis of Cu₂ZnSnS₄ Nanocrystals through Cation Exchange for Photovoltaic Devices. *Chem. Mater.* **2014**, *26*, 5492–5498
- (4) Oh, N.; Kim, B. H.; Cho, S.-Y.; Nam, S.; Rogers, S. P.; Jiang, Y.; Flanagan, J. C.; Zhai, Y.; Kim, J.-H.; Lee, J.; Yu, Y.; Cho, Y. K.; Hur, G.; Zhang, J.; Trefonas, P.; Rogers, J. A.; Shim, M. Double-Heterojunction Nanorod Light-Responsive LEDs for Display Applications. *Science* **2017**, *355*, 616–619.
- (5) Panfil, Y. E.; Oded, M.; Banin, U. Colloidal Quantum Nanostructures: Emerging Materials for Display Applications. *Angew. Chem. Int. Ed.* **2018**, *57*, 4274–4295.
- (6) Han, S.; Qin, X.; An, Z.; Zhu, Y.; Liang, L.; Han, Y.; Huang, W.; Liu, X. Multicolour Synthesis in Lanthanide-Doped Nanocrystals through Cation Exchange in Water. *Nat. Commun.* **2016**, *7*, 1–7.
- (7) Zhou, J.; Liu, Q.; Feng, W.; Sun, Y.; Li, F. Upconversion Luminescent Materials: Advances and Applications. *Chem. Rev.* **2015**, *115*, 395–465.
- (8) Teitelboim, A.; Meir, N.; Kazes, M.; Oron, D. Colloidal Double Quantum Dots. *Acc. Chem. Res.* **2016**, *49*, 902–910.
- (9) De Trizio, L.; Manna, L. Forging Colloidal Nanostructures *via* Cation Exchange Reactions. *Chem. Rev.* **2016**, *116*, 10852–10887.
- (10) Beberwyck, B. J.; Surendranath, Y.; Alivisatos, A. P. Cation Exchange: A Versatile Tool for Nanomaterials Synthesis. *J. Phys. Chem. C* **2013**, *117*, 19759–19770.
- (11) Luther, J. M.; Zheng, H.; Sadtler, B.; Alivisatos, A. P. Synthesis of PbS Nanorods and Other Ionic Nanocrystals of Complex Morphology by Sequential Cation Exchange Reactions. *J. Am. Chem. Soc.* **2009**, *131*, 16851–16857.
- (12) Akkerman, Q. A.; Genovese, A.; George, C.; Prato, M.; Moreels, I.; Casu, A.; Marras, S.; Curcio, A.; Scarpellini, A.; Pellegrino, T.; Manna, L.; Lesnyak, V. From Binary Cu₂S to Ternary Cu–In–S and Quaternary Cu–In–Zn–S Nanocrystals with Tunable Composition *via* Partial Cation Exchange. *ACS Nano* **2015**, *9*, 521–531.
- (13) Powell, A. E.; Hodges, J. M.; Schaak, R. E. Preserving Both Anion and Cation Sublattice Features during a Nanocrystal Cation-Exchange Reaction: Synthesis of Metastable Wurtzite-Type CoS and MnS. *J. Am. Chem. Soc.* **2016**, *138*, 471–474.
- (14) Li, H.; Zanella, M.; Genovese, A.; Povia, M.; Falqui, A.; Giannini, C.; Manna, L. Sequential Cation Exchange in Nanocrystals: Preservation of Crystal Phase and Formation of Metastable Phases. *Nano Lett.* **2011**, *11*, 4964–4970.
- (15) Jain, P. K.; Amirav, L.; Aloni, S.; Alivisatos, A. P. Nanoheterostructure Cation Exchange: Anionic Framework Conservation. *J. Am. Chem. Soc.* **2010**, *132*, 9997–9999.
- (16) Fenton, J. L.; Steimle, B. C.; Schaak, R. E. Tunable Intraparticle Frameworks for Creating Complex Heterostructured Nanoparticle Libraries. *Science* **2018**, *360*, 513–517.
- (17) Liu, Y.; Liu, M.; Yin, D.; Qiao, L.; Fu, Z.; Swihart, M. T. Selective Cation Incorporation into Copper Sulfide Based Nanoheterostructures. *ACS Nano* **2018**, *12*, 7803–7811.
- (18) Steimle, B. C.; Fenton, J. L.; Schaak, R. E. Rational Construction of a Scalable Heterostructured Nanorod Megalibrary. *Science* **2020**, *367*, 418–424.
- (19) Fenton, J. L.; Steimle, B. C.; Schaak, R. E. Structure-Selective Synthesis of Wurtzite and Zincblende ZnS, CdS, and CuInS2 Using Nanoparticle Cation Exchange Reactions. *Inorg. Chem.* **2019**, *58*, 672–678.

- (20) Fenton, J. L.; Schaak, R. E. Structure-Selective Cation Exchange in the Synthesis of Zincblende MnS and CoS Nanocrystals. *Angew. Chem. Int. Ed.* **2017**, *56*, 6464–6467.
- (21) Fenton, J. L.; Steimle, B.; Schaak, R. E. Exploiting Crystallographic Regioselectivity to Engineer Asymmetric Three-Component Colloidal Nanoparticle Isomers Using Partial Cation Exchange Reactions. *J. Am. Chem. Soc.* **2018**, *140*, 6771–6775.
- (22) Sadtler, B.; Demchenko, D. O.; Zheng, H.; Hughes, S. M.; Merkle, M. G.; Dahmen, U.; Wang, L.-W.; Alivisatos, A. P. Selective Facet Reactivity during Cation Exchange in Cadmium Sulfide Nanorods. *J. Am. Chem. Soc.* **2009**, *131*, 5285–5293.
- (23) Bothe, C.; Kornowski, A.; Tornatzky, H.; Schmidtke, C.; Lange, H.; Maultzsch, J.; Weller, H. Solid-State Chemistry on the Nanoscale: Ion Transport through Interstitial Sites or Vacancies? *Angew. Chem. Int. Ed.* **2015**, *54*, 14183–14186.
- (24) Casavola, M.; van Huis, M. A.; Bals, S.; Lambert, K.; Hens, Z.; Vanmaekelbergh, D. Anisotropic Cation Exchange in PbSe/CdSe Core/Shell Nanocrystals of Different Geometry. *Chem. Mater.* **2012**, *24*, 294–302.
- (25) Lesnyak, V.; Brescia, R.; Messina, G. C.; Manna, L. Cu Vacancies Boost Cation Exchange Reactions in Copper Selenide Nanocrystals. *J. Am. Chem. Soc.* **2015**, *137*, 9315–9323.
- (26) Gariano, G.; Lesnyak, V.; Brescia, R.; Bertoni, G.; Dang, Z.; Gaspari, R.; De Trizio, L.; Manna, L. Role of the Crystal Structure in Cation Exchange Reactions Involving Colloidal Cu₂Se Nanocrystals. *J. Am. Chem. Soc.* **2017**, *139*, 9583–9590.
- (27) Hernández-Pagán, E. A.; O'Hara, A.; Arrowood, S. L.; McBride, J. R.; Rhodes, J. M.; Pantelides, S. T.; Macdonald, J. E. Transformation of the Anion Sublattice in the Cation-Exchange Synthesis of Au₂S from Cu_{2-x}S Nanocrystals. *Chem. Mater.* **2018**, *30*, 8843–8851.
- (28) Gates-Rector, S.; Blanton, T. The Powder Diffraction File: A Quality Materials Characterization Database. *Powder Diffr.* **2019**, 34, 352–360.
- (29) Morimoto, N.; Kullerud, G. Polymorphism in Digenite. *Am. Mineral.* **1963**, 48, 110–123.
- (30) Will, G.; Hinze, E.; Abdelrahman, A. R. M. Crystal Structure Analysis and Refinement of Digenite, Cu_{1.8}S, in the Temperature Range 20 to 500 C under Controlled Sulfur Partial Pressure. *Eur. J. Mineral.* **2002**, *14*, 591–598.
- (31) Donnay, G.; Donnay, J. D. H.; Kullerud, G. Crystal and Twin Structure of Digenite, Cu₉S₅. Am. Mineral. 1958, 43, 228–242.

- (32) Kashida, S.; Yamamoto, K. An X-Ray Study of the Incommensurate Structure in Digenite (Cu_{1.8}S). *J. Phys. Condens. Matter* **1991**, *3*, 6559–6570
- (33) Ge, S.; Wong, K. W.; Ng, K. M. Revitalizing Digenite Cu_{1.8}S Nanoparticles with the Localized Surface Plasmon Resonance (LSPR) Effect by Manganese Incorporation. *New J. Chem.* **2017**, *41*, 677–684.
- (34) Lotfipour, M.; Machani, T.; Rossi, D. P.; Plass, K. E. α-Chalcocite Nanoparticle Synthesis and Stability. *Chem. Mater.* **2011**, *23*, 3032–3038.
- (35) Liu, L.; Zhong, H.; Bai, Z.; Zhang, T.; Fu, W.; Shi, L.; Xie, H.; Deng, L.; Zou, B. Controllable Transformation from Rhombohedral Cu_{1.8}S Nanocrystals to Hexagonal CuS Clusters: Phase- and Composition-Dependent Plasmonic Properties. *Chem. Mater.* **2013**, *25*, 4828–4834.
- (36) Sines, I. T.; Schaak, R. E. Phase-Selective Chemical Extraction of Selenium and Sulfur from Nanoscale Metal Chalcogenides: A General Strategy for Synthesis, Purification, and Phase Targeting. *J. Am. Chem. Soc.* **2011**, 133, 1294–1297.
- (37) Nelson, A.; Ha, D.-H.; Robinson, R. D. Selective Etching of Copper Sulfide Nanoparticles and Heterostructures through Sulfur Abstraction: Phase Transformations and Optical Properties *Chem. Mater.* **2016**, *28*, 8530-8541.
- (38) Coughlan, C.; Ibáñez, M.; Dobrozhan, O.; Singh, A.; Cabot, A.; Ryan, K. M. Compound Copper Chalcogenide Nanocrystals. *Chem. Rev.* **2017**, *117*, 5865-6109.
- (39) Liu, L.; Liu, C.; Fu, W.; Deng, L.; Zhong, H. Phase Transformations of Copper Sulfide Nanocrystals: Towards Highly Efficient Quantum-Dot-Sensitized Solar Cells. *ChemPhysChem* **2016**, *17*, 771–776.
- (40) Tappan, B. A.; Barim, G.; Kwok, J. C.; Brutchey, R. L. Utilizing Diselenide Precursors toward Rationally Controlled Synthesis of Metastable CuInSe₂ Nanocrystals. *Chem. Mater.* **2018**, *30*, 5704–5713.
- (41) Tappan, B. A.; Horton, M. K.; Brutchey, R. L. Ligand-Mediated Phase Control in Colloidal AgInSe₂ Nanocrystals. *Chem. Mater.* **2020**, *32*, 2935–2945.
- (42) Ha, D.-H.; Caldwell, A. H.; Ward, M. J.; Honrao, S.; Mathew, K.; Hovden, R.; Koker, M. K. A.; Muller, D. A.; Hennig, R. G.; Robinson, R. D. Solid–Solid Phase Transformations Induced through Cation Exchange and Strain in 2D Heterostructured Copper Sulfide Nanocrystals. *Nano Lett.* **2014**, *14*, 7090–7099.

